The Prediction of Pharmacokinetic Properties of Compounds in *Hemigraphis alternata* (Burm.F.) T. Ander Leaves Using pkCSM

Yeni Yeni* and Rizky Arcinthya Rachmania

Department of Pharmacy, Universitas Muhammadiyah Prof. DR. HAMKA, Jl. Delima II/IV, Jakarta 13460, Indonesia

Abstract: *The inflammatory process aids in healing and maintains the body's balance. Untreated acute inflammation can cause organ disease, which can lead to a chronic inflammatory phenotype.* Hemigraphis alternata *is a plant that has anti-inflammatory activity. The compounds contained in* H. alternata *leaves have been predicted to have an affinity for receptors involved in the inflammatory process. A large number of drug candidates were withdrawn from preclinical trials due to their poor pharmacokinetic profiles. Drug compounds must cross the barriers that exist in the body to reach their biological targets so that they can generate a biological effect. The pharmacokinetic features of 22 components in* H. alternata *leaves were predicted in order to search for inflammatory medication candidates with suitable pharmacokinetic profiles. The pkCSM, a strategy for predicting and optimizing the pharmacokinetic properties of small molecules based on distance-based graph signatures was used in this work. The pkCSM employed 20 predictors separated into four groups: absorption, distribution, metabolism, and excretion. Based on the prediction findings, there are five substances with the best pharmacokinetic features, 8a-methyl-3,4,4a,5,6,7-hexahydro-2H-naphthalene-1,8-dione, (E)-3,7,11,15-tetramethylhexadec-2-en-1-ol, 2-methylenecholestan-3-ol, 5-(hydroxymethyl) furan-2-carbaldehyde and 2,3-dihydro-2,5-dimethyl-5H-1,4-dioxepin.*

Keywords: *Hemigraphis alternata; pharmacokinetic profiles; pkCSM*

■ INTRODUCTION

Inflammation is the body's defensive reaction to potentially hazardous impulses such as viruses or chemicals that induce cell injury. It triggers inflammatory cells and signaling pathways. The inflammation process is critical in the recovery process because it allows aberrant bodily homeostasis to be restored. Acute inflammation that is not effectively managed can aggravate organ disease and eventually develop into a chronic inflammatory phenotype [1-3].

Hemigraphis alternata possesses anti-nociceptive, anti-inflammatory, and anti-diarrheal effects. In mice, ethyl acetate and methanol extracts of *H. alternata* leaves were found to exhibit anti-inflammatory and non-toxic effects [4]. This plant's leaves contain 22 secondary metabolites (Fig. 1) [5]. These substances exhibit anti-inflammatory effects against cyclooxygenase-1 (COX-1) and 5-lipoxygenase (5-LOX) receptors [6-7].

The interaction of pharmacokinetic characteristics, toxicity, and potency significantly impacts a drug's efficacy. A compound's pharmacokinetic profiles are determined to assess its absorption, distribution, metabolism, and excretion (ADME) features [8]. The preliminary evaluation of ADME features will assist pharmaceutical researchers in selecting the best medication candidates for development and rejecting drug candidates with a poor likelihood of success [9]. Creating novel drug candidates is a challenging, time-consuming, and expensive procedure. In developing novel medications, *in silico* computational model plays an essential role. Its use reduces the amount of time and resources needed for the rational design of novel medication candidates. Pharmaceutical advancements have raised the necessity for more accurate methodologies to predict the pharmacokinetic features of novel drug candidates. Because of the improvement of

1082

Indones. J. Chem., 2022, 22 (4), 1081 - 1089
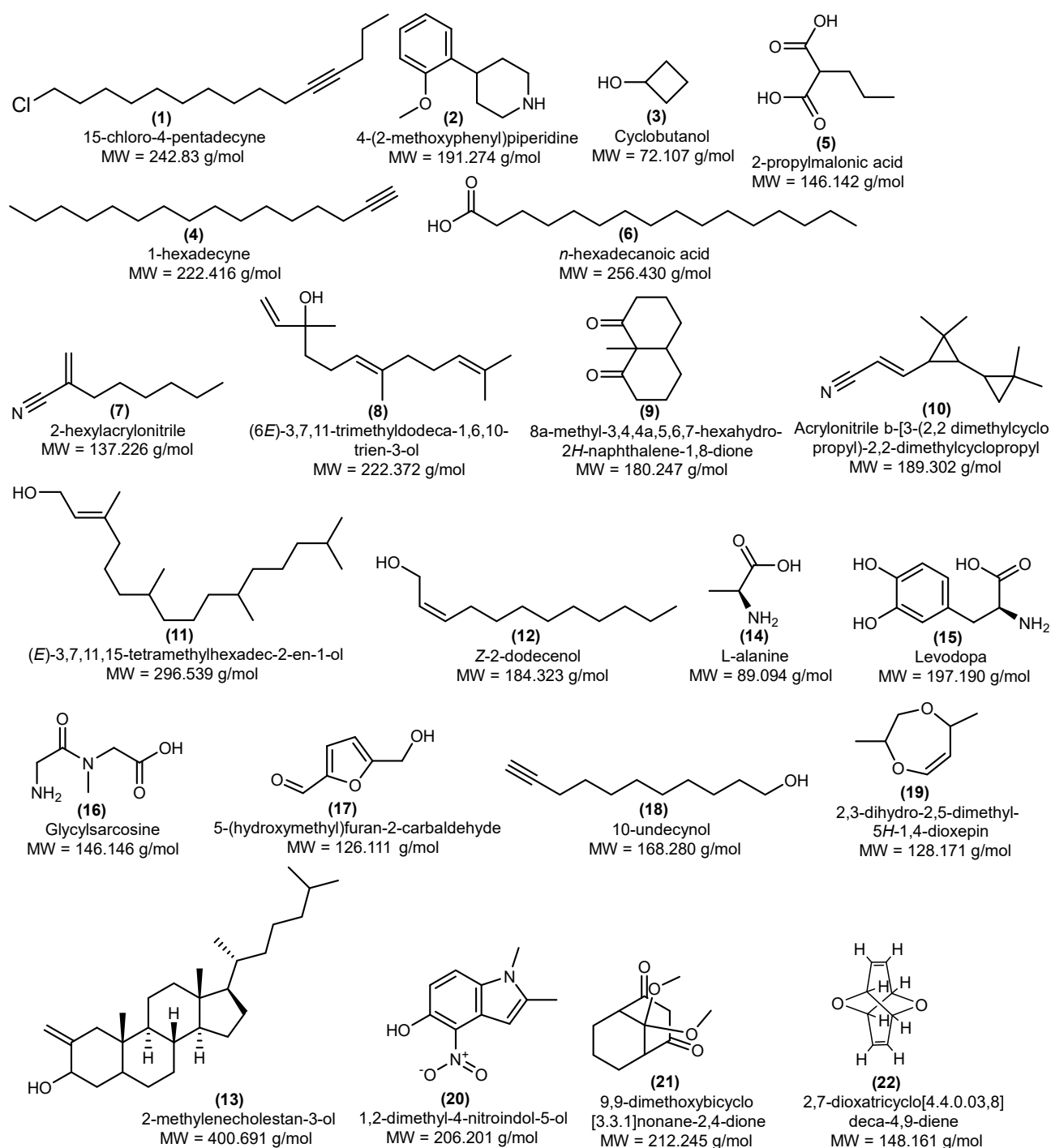
Fig 1. The compounds contained in *H. alternata* leaves [6-7]

(1)
15-chloro-4-pentadecyne
MW = 242.83 g/mol

(2)
4-(2-methoxyphenyl)piperidine
MW = 191.274 g/mol

(3)
Cyclobutanol
MW = 72.107 g/mol

(5)
2-propylmalonic acid
MW = 146.142 g/mol

(4)
1-hexadecyne
MW = 222.416 g/mol

(6)
n-hexadecanoic acid
MW = 256.430 g/mol

(7)
2-hexylacrylonitrile
MW = 137.226 g/mol

(8)
(6*E*)-3,7,11-trimethyldodeca-1,6,10-
trien-3-ol
MW = 222.372 g/mol

(9)
8a-methyl-3,4,4a,5,6,7-hexahydro-
2*H*-naphthalene-1,8-dione
MW = 180.247 g/mol

(10)
Acrylonitrile b-[3-(2,2 dimethylcyclo
propyl)-2,2-dimethylcyclopropyl
MW = 189.302 g/mol

(11)
(*E*)-3,7,11,15-tetramethylhexadec-2-en-1-ol
MW = 296.539 g/mol

(12)
Z-2-dodecenol
MW = 184.323 g/mol

(14)
L-alanine
MW = 89.094 g/mol

(15)
Levodopa
MW = 197.190 g/mol

(16)
Glycylsarcosine
MW = 146.146 g/mol

(17)
5-(hydroxymethyl)furan-2-carbaldehyde
MW = 126.111 g/mol

(18)
10-undecynol
MW = 168.280 g/mol

(19)
2,3-dihydro-2,5-dimethyl-
5*H*-1,4-dioxepin
MW = 128.171 g/mol

(13)
2-methylenecholestan-3-ol
MW = 400.691 g/mol

(20)
1,2-dimethyl-4-nitroindol-5-ol
MW = 206.201 g/mol

(21)
9,9-dimethoxybicyclo
[3.3.1]nonane-2,4-dione
MW = 212.245 g/mol

(22)
2,7-dioxatricyclo[4.4.0.03,8]
deca-4,9-diene
MW = 148.161 g/mol

computer algorithms and massive information databases, computational prediction tools are increasingly routinely employed in the procedure for drug discovery. Furthermore, *in silico* technologies have been employed to discover various drugs that are now used in the treatment of disorders [10-13].

The pkCSM is a tool that can characterize the pharmacokinetic profile of compounds comprehensively. The concept used to predict the predictors by this tool is graph-based structural

signatures which train the prediction algorithm by encoding the pattern of distances between atoms. Graphical modeling results from an understandable and well-established mathematical description of chemical entities. Different predictors, including molecular structure and chemistry, may be retrieved using pkCSM [14-16]. Despite the diversity in the size of the data set and the distribution of experimental values, the pkCSM model was able to establish a strong correlation with experimental results through regression analysis of the ADME predictors [8]. The mission of *in silico* ADME prediction is to accurately forecast the *in vivo* pharmacokinetic features of prospective therapeutic compounds in humans using only virtual structures. In this work, *in silico* analysis was used to estimate the pharmacokinetic features of 22 chemicals found in *H. alternata* leaves.

■ EXPERIMENTAL SECTION

Materials

PubChem (pubchem.ncbi.nlm.nih.gov) provided the SMILES format of 22 chemicals found in the leaves of *H. alternata*. The SMILES translator, cactus in https://cactus.nci.nih.gov can be used to get compounds that do not have the SMILES format in PubChem.

Instrumentation

The pharmacokinetic characteristics of 22 chemicals in the leaves of *H. alternata* were estimated using pkCSM (http://biosig.unimelb.edu.au/pkcsm/prediction).

Procedure

The application of pkCSM is based on general compound qualities (molecular properties, toxicophores, and pharmacophores), as well as distance-based graph signatures. In pkCSM, there are 20 predictors that describe the pharmacokinetic properties of a compound. The predictors were divided into the absorption of 7 predictors, distribution of 4 predictors, metabolism of 7 predictors, and excretion of 2 predictors (Table 1) [8,17-18].

In this study, virtual screening was carried out to obtain several compounds that had good ADME. The findings of the ADME predictor, which has a numerical value with specific constraints, are used in virtual screening. Caco-2 permeability (A2), intestinal absorption

Table 1. Distribution of ADME predictors in pkCSM [8]

Pharmacokinetic parameter	Predictor (code)	Unit	Requirement value
Absorption	Water solubility (A1)	log mol/L	-
	Caco-2 permeability (A2)	log Papp in 10^{-6} cm/s	> 0.9
	Intestinal absorption (human) (A3)	% Absorbed	> 30%
	Skin permeability (A4)	log Kp	≥ -2.5
	P-glycoprotein substrate (A5)	Yes/No	-
	P-glycoprotein I inhibitor (A6)	Yes/No	-
	P-glycoprotein II inhibitor (A7)	Yes/No	-
Distribution	VDss (human) (D1)	log L/kg	≥ -0.15
	Fraction unbound (human) (D2)	Fu	-
	BBB permeability (D3)	log BB	≥ -1
	CNS permeability (D4)	log PS	≥ -3
Metabolism	CYP2D6 substrate (M1)	Yes/No	-
	CYP3A4 substrate (M2)	Yes/No	-
	CYP1A2 inhibitor (M3)	Yes/No	-
	CYP2C19 inhibitor (M4)	Yes/No	-
	CYP2C9 inhibitor (M5)	Yes/No	-
	CYP2D6 inhibitor (M6)	Yes/No	-
	CYP3A4 inhibitor (M7)	Yes/No	-
Excretion	Total clearance (E1)	log mL/min/kg	Higher is better
	Renal OCT2 substrate (E2)	Yes/No	-

1084

Indones. J. Chem., 2022, 22 (4), 1081 - 1089

(human) (A3), skin permeability (A4), the human volume of distribution at steady state (VDss) (D1), Blood-Brain Barrier (BBB) permeability (D3), Central Nervous System (CNS) permeability (D4), and total clearance were the predictors (E1) [19].

Initially, test compounds were selected based on predictors of Caco-2 permeability (A2), intestinal absorption (human) (A3), skin permeability (A4), VDss (human) (D1), BBB permeability (D3), and CNS permeability (D4). The compounds that meet the requirements will be re-screened based on the highest total clearance (E1) value [8].

■ RESULTS AND DISCUSSION

The use of pkCSM is a strategy for estimating and improving the pharmacokinetic characteristics of small compounds based on distance-based graph signatures. The use of pkCSM extends the cutoff scanning idea to depict molecular and chemical structures in order to characterize and predict their pharmacokinetic features [8].

Water solubility is an essential aspect in a drug's pharmacological reaction following oral delivery. Drugs with strong water solubility will have good absorption and bioavailability qualities. Drug absorption and bioavailability can boost plasma drug concentrations at the target location, allowing it to fulfill therapeutic actions [20].

Caco-2 cells are a kind of colorectal cancer cell line [21]. In preclinical studies, the Caco-2 model was utilized to predict medication gastrointestinal permeability. Based on the properties of the human small intestine, this model expresses enterocytes, transporters, cytochrome P450 enzymes and microvilli [22]. A compound's Caco-2 permeability is high if its Papp is more than 8×10^{-6} cm/s.

The gut is the primary location of oral medication absorption. The skin serves as a barrier between the interior and exterior environments of the body. Skin qualities and traits can vary and influence medication distribution and toxicity [23]. The skin permeability constant log Kp (cm/h) expresses a compound's likelihood to be skin permeable.

P-glycoprotein (P-gp) is an ATP-binding cassette (ABC) transporter that acts as a biological barrier in cells by eliminating toxins and xenobiotics. The ability of a chemical to block the transport of P-gp I and P-gp II is referred to as P-gp I/II inhibitor. P-gp-mediated transport modification has important pharmacokinetic consequences for P-gp substrates. Inhibiting P-gp I or P-gp II might provide therapeutic benefits or result in contraindications [8].

VDss (human) is calculated by dividing all drugs inside the body by drug concentration in plasma in a stable state. This state happens when the system receives a consistent rate of medication infusion into the plasma, and all drug concentrations in the body remain constant [24]. The capacity of medicine to bind proteins in the blood can have an impact on its efficacy. The greater the proportion of the drug that is not bound to protein (fraction unbound), the more effectively the medication will cross or diffuse through the cell membrane [8].

Increased permeability of the BBB, a physical and biochemical barrier that plays a role in the protection of cerebral homeostasis, can alter the pathological development of ischemic tissue [25-26]. The value of the blood-brain permeability surface area product can be used to estimate a pharmacological compound's capacity to reach the CNS (log PS). This value was achieved through *in situ* brain perfusion with the chemical directly injected into the carotid artery without any systemic distribution impact that may skew brain penetration [8].

Cytochrome P450 is a detoxifying enzyme present in the liver. In general, cytochrome P450 is involved in drug metabolism. However, P450 inhibitors can significantly affect medication pharmacokinetics. As a result, it is critical to determine if the provided molecule is a CYP2D6/CYP3A4 substrate expected to be processed by P450. Cytochrome P450 oxidizes xenobiotics so that they can be excreted. Many medications are inactivated by cytochrome P450, whereas others might be activated by it. These enzyme inhibitors have the potential to interfere with medication metabolism and are thus not recommended. Therefore, it is critical to evaluate the compound's capacity to inhibit cytochrome P450 (isoforms CYP1A2/CYP2C19/CYP2C9/CYP2D6/CYP3A4). A substance is termed a cytochrome P450 inhibitor if the

concentration required to achieve 50% inhibition is less than 10 M [8].

The amount of drug removed from plasma in the vascular compartment per unit time is referred to as drug clearance. Total clearance is the result of all body clearances. Total clearance indicates drug removal from the core compartment without regard for the process mechanism [27]. The renal uptake transporter Organic Cation Transporter 2 (OCT2) is crucial for the disposition of drugs and renal clearance. When used with OCT2 inhibitors, OCT2 substrates might have negative side effects [8].

In the results of the prediction of absorption properties obtained compounds 3, 6, 9, 11, 13, 17, 19, 20, 21, and 22, which are in accordance with the requirements (Table 2). Meanwhile, the compounds that

Table 2. The prediction results of absorption properties 22 compounds contained in *H. alternata* using pkCSM

No	Compound	MW	A1	A2	A3	A4	A5	A6	A7
1	15-chloro-4-pentadecyne	242.830	-7.634	1.402	92.577	-2.420	No	No	No
2	4-(2-methoxyphenyl)piperidine	191.274	-1.835	1.385	91.872	-2.283	No	No	No
3	Cyclobutanol	72.107	0.092	1.463	98.450	-3.027	Yes	No	No
4	1-hexadecyne	222.416	-7.801	1.382	92.797	-2.225	No	No	No
5	2-propylmalonic acid	146.142	-1.323	0.667	74.589	-2.735	No	No	No
6	*n*-hexadecanoic acid	256.430	-5.562	1.558	92.004	-2.717	No	No	No
7	2-hexylacrylonitrile	137.226	-3.861	1.357	94.383	-1.278	No	No	No
8	(6*E*)-3,7,11-trimethyldodeca-1,6,10-trien-3-ol	222.372	-5.176	1.498	91.887	-1.477	No	No	No
9	8a-methyl-3,4,4a,5,6,7-hexahydro-2*H*-naphthalene-1,8-dione	180.247	-2.187	1.605	97.468	-2.814	No	No	No
10	Acrylonitrile β-[3-(2,2-dimethylcyclopropyl)-2,2-dimethylcyclopropyl	189.302	-4.729	1.382	95.941	-1.606	No	No	No
11	(*E*)-3,7,11,15-tetramethylhexadec-2-en-1-ol	296.539	-7.554	1.515	90.710	-2.576	No	No	Yes
12	*Z*-2-dodecenol	184.323	-4.816	1.474	91.684	-1.529	No	No	No
13	2-methylenecholestan-3-ol	400.691	-5.818	1.208	95.328	-2.733	No	No	Yes
14	L-alanine	89.094	-2.887	0.466	81.091	-2.738	No	No	No
15	Levodopa	197.190	-2.890	-0.289	47.741	-2.735	Yes	No	No
16	Glycylsarcosine	146.146	-2.699	0.545	68.130	-2.735	No	No	No
17	5-(hydroxymethyl)furan-2-carbaldehyde	126.111	-0.590	1.172	95.848	-3.416	No	No	No
18	10-undecynol	168.280	-3.892	1.476	93.273	-1.448	No	No	No
19	2,3-dihydro-2,5-dimethyl-5*H*-1,4-dioxepin	128.171	-0.757	1.621	97.700	-2.878	No	No	No
20	1,2-dimethyl-4-nitroindol-5-ol	206.201	-2.799	0.903	92.210	-2.622	No	No	No
21	9,9-dimethoxybicyclo[3.3.1]nonane-2,4-dione	212.245	-1.452	1.237	100	-3.221	No	No	No
22	2,7-dioxatricyclo[4.4.0.03,8]deca-4,9-diene	148.161	-1.632	1.563	100	-3.097	No	No	No

Note: ▨ = The compounds that satisfy the requirement values, MW = Molecular Weight (g/mol), A1 = Water solubility, A2 = Caco2 permeability, A3 = Intestinal absorption (human), A4 = Skin Permeability, A5 = P-glycoprotein substrate, A6 = P-glycoprotein I inhibitor, A7 = P-glycoprotein II inhibitor

1086

Indones. J. Chem., 2022, 22 (4), 1081 - 1089

meet the requirements for distribution and excretion properties are compounds 1, 2, 4, 7, 8, 9, 11, 12, 13, 17, 18, and 19 (Table 3). Therefore, the compounds 9 (8a-methyl-3,4,4a,5,6,7-hexahydro-2*H*-naphthalene-1,8-dione), 11 ((*E*)-3,7,11,15-tetramethylhexadec-2-en-1-ol), 13 (2-methylenecholestan-3-ol), 17 (5-(hydroxymethyl) furan-2-carbaldehyde) and 19 (2,3-dihydro-2,5-dimethyl-5*H*-1,4-dioxepin) can be used as anti-inflammatory drug candidates that have good ADME because these

compounds are intersection which meet the requirements of absorption, distribution and excretion predictors. Prediction of the metabolism properties of these 22 compounds provides information about the possibility of these compounds being metabolized in the liver. There are 2 compounds from 5 virtual screening compounds that are predicted to be metabolized in the liver. Compound 11 is a CYP3A4 substrate (M2) and a CYP1A2 inhibitor (M3), while compound 13 is a CYP3A4

Table 3. The prediction results of distribution and excretion properties 22 compounds contained in *H. alternata* using pkCSM

No	Compound	D1	D2	D3	D4	E1	E2
1	15-chloro-4-pentadecyne	0.534	0.062	0.917	-1.257	0.557	No
2	4-(2-methoxyphenyl)piperidine	1.122	0.462	0.502	-2.260	0.880	No
3	Cyclobutanol	0.047	0.762	-0.031	-2.820	0.448	No
4	1-hexadecyne	0.631	0.067	0.956	-1.364	1.870	No
5	2-propylmalonic acid	-0.936	0.588	-0.060	-3.023	0.444	No
6	*n*-hexadecanoic acid	-0.543	0.101	-0.111	-1.816	1.763	No
7	2-hexylacrylonitrile	0.260	0.414	0.571	-1.976	0.550	No
8	(6*E*)-3,7,11-trimethyldodeca-1,6,10-trien-3-ol	0.370	0.234	0.652	-2.093	1.739	No
9	8a-methyl-3,4,4a,5,6,7-hexahydro-2*H*-naphthalene-1,8-dione	0.191	0.564	0.447	-2.813	1.266	No
10	Acrylonitrile β-[3-(2,2-dimethylcyclopropyl)-2,2-dimethylcyclopropyl	0.531	0.271	0.609	-1.923	0.120	No
11	(*E*)-3,7,11,15-tetramethylhexadec-2-en-1-ol	0.468	0	0.806	-1.563	1.686	No
12	*Z*-2-dodecenol	0.358	0.275	0.713	-1.902	1.781	No
13	2-methylenecholestan-3-ol	-0.145	0	0.808	-1.411	0.546	No
14	L-alanine	-0.534	0.473	-0.412	-3.405	0.370	No
15	Levodopa	-0.105	0.604	-0.843	-3.032	0.430	No
16	Glycylsarcosine	-0.680	0.538	-0.614	-3.183	0.217	No
17	5-(hydroxymethyl)furan-2-carbaldehyde	-0.146	0.744	-0.361	-2.914	0.614	No
18	10-undecynol	0.300	0.353	0.721	-1.957	1.713	No
19	2,3-dihydro-2,5-dimethyl-5*H*-1,4-dioxepin	-0.007	0.692	0.014	-2.842	0.569	No
20	1,2-dimethyl-4-nitroindol-5-ol	0.209	0.207	-0.263	-2.106	0.537	No
21	9,9-dimethoxybicyclo[3.3.1]nonane-2,4-dione	0.015	0.617	-0.217	-2.909	0.198	No
22	2,7-dioxatricyclo[4.4.0.03,8]deca-4,9-diene	0.558	0.678	-0.01	-3.357	0.135	No

Note: ▨ = The compounds that satisfy the requirement values, D1 = VDss (human), D2 = Fraction unbound (human), D3 = BBB permeability, D4 = CNS permeability, E1 = Total Clearance, E2 = Renal OCT2 substrate

Table 4. The prediction results of metabolism properties 22 compounds contained in *H. alternata* using pkCSM

No	Compound	M1	M2	M3	M4	M5	M6	M7
1	15-chloro-4-pentadecyne	No	Yes	Yes	No	No	No	No
2	4-(2-methoxyphenyl)piperidine	No	No	No	No	No	No	No
3	Cyclobutanol	No	No	No	No	No	No	No
4	1-hexadecyne	No	Yes	Yes	No	No	No	No
5	2-propylmalonic acid	No	No	No	No	No	No	No
6	*n*-hexadecanoic acid	No	Yes	No	No	No	No	No
7	2-hexylacrylonitrile	No	No	No	No	No	No	No
8	(6*E*)-3,7,11-trimethyldodeca-1,6,10-trien-3-ol	No	No	No	No	No	No	No
9	8a-methyl-3,4,4a,5,6,7-hexahydro-2*H*-naphthalene-1,8-dione	No	No	No	No	No	No	No
10	Acrylonitrile β-[3-(2,2-dimethylcyclopropyl)-2,2-dimethylcyclopropyl	No	No	No	No	No	No	No
11	(*E*)-3,7,11,15-tetramethylhexadec-2-en-1-ol	No	Yes	Yes	No	No	No	No
12	*Z*-2-dodecenol	No	No	No	No	No	No	No
13	2-methylenecholestan-3-ol	No	Yes	No	No	No	No	No
14	L-alanine	No	No	No	No	No	No	No
15	Levodopa	No	No	No	No	No	No	No
16	Glycylsarcosine	No	No	No	No	No	No	No
17	5-(hydroxymethyl)furan-2-carbaldehyde	No	No	No	No	No	No	No
18	10-undecynol	No	No	No	No	No	No	No
19	2,3-dihydro-2,5-dimethyl-5H-1,4-dioxepin	No	No	No	No	No	No	No
20	1,2-dimethyl-4-nitroindol-5-ol	No	No	Yes	No	No	No	No
21	9,9-dimethoxybicyclo[3.3.1]nonane-2,4-dione	No	No	No	No	No	No	No
22	2,7-dioxatricyclo[4.4.0.03,8]deca-4,9-diene	No	No	No	No	No	No	No

Note: ▨ = The selected compounds, M1 = CYP2D6 substrate, M2 = CYP3A4 substrate, M3 = CYP1A2 inhibitor, M4 = CYP2C19 inhibitor, M5 = CYP2C9 inhibitor, M6 = CYP2D6 inhibitor, M7= CYP3A4 inhibitor

substrate (M2) (Table 4). The basic structures of the five drugs projected to have favorable pharmacokinetic characteristics differ. However, several of them share the same substituents. Compounds 9, 11, 13, and 19 all contain methyl substituents. Compounds 11, 13, and 17 all contain hydroxyl substituents. In this study, the screening process was based on predictors which had a limited value to determine whether or not the pharmacokinetic profile of a compound was good. The predictors included Caco-2 permeability (A2), intestinal absorption (human) (A3),

skin permeability (A4), VDss (human) (D1), BBB permeability (D3) and CNS permeability (D4). The results of the virtual screening were then sorted based on the highest total clearance value (E1) log mL/min/kg, in this study ≥ 0.54.

■ **CONCLUSION**

There are five chemicals in *Hemigraphis alternata* leaves that are projected to have the best pharmacokinetic qualities, 8a-methyl-3,4,4a,5,6,7-

hexahydro-2*H*-naphthalene-1,8-dione, (*E*)-3,7,11,15-tetramethylhexadec-2-en-1-ol, 2-methylenecholestan-3-ol, 5-(hydroxymethyl) furan-2-carbaldehyde and 2,3-dihydro-2,5-dimethyl-5*H*-1,4-dioxepin. These compounds met the most absorption, distribution, and excretion predictors requirements compared to other compounds.

■ AUTHOR CONTRIBUTIONS

YY and RAR conducted the experiment, YY conducted the conceptualization, methodology, formal analysis, writing, review, and editing, and RAR conducted data curation and writing-original draft preparation.

■ REFERENCES

[1] Chen, L., Deng, H., Cui, H., Fang, J., Zuo, Z., Deng, J., Li, Y., Wang, X., and Zhao, L., 2018, Inflammatory responses and inflammation-associated diseases in organs, *Oncotarget*, 9 (6), 7204–7218.

[2] Antonelli, M., and Kushner, I., 2017, It's time to redefine inflammation, *FASEB J.*, 31 (5), 1787–1791.

[3] Serhan, C.N., Gupta, S.K., Perretti, M., Godson, C., Brennan, E., Li, Y., Soehnlein, O., Shimizu, T., Werz, O., Chiurchiù, V., Azzi, A., Dubourdeau, M., Gupta, S.S., Schopohl, P., Hoch, M., Gjorgevikj, D., Khan, F.M., Brauer, D., Tripathi, A., Cesnulevicius, K., Lescheid, D., Schultz, M., Särndahl, E., Repsilber, D., Kruse, R., Sala, A., Haeggström, J.Z., Levy, B.D., Filep, J.G., and Wolkenhauer, O., 2020, The atlas of inflammation resolution (AIR), *Mol. Aspects Med.*, 74, 100894.

[4] Rahman, S.M.M., Atikullah, M., Islam, M.N., Mohaimenul, M., Ahammad, F., Islam, M.S., Saha, B., and Rahman, M.H., 2019, Anti-inflammatory, antinociceptive and antidiarrhoeal activities of methanol and ethyl acetate extract of *Hemigraphis alternata* leaves in mice, *Clin. Phytosci.*, 5 (1), 16.

[5] Ming, W.K., 2019, Bioassay-guided purification and identification of chemical constituents from *Hemigraphis alternata*, *Dissertation*, Monash University, Malaysia.

[6] Yeni, Y., Rachmania, R.A., and Mochamad, D.Y.M., 2021, Affinity of compounds in *Hemigraphis alternata* (Burm.F.) T. Ander leaves to cyclooxygenase 1 (COX-1): *In silico* approach, *Proceedings of the 4th International Conference on Sustainable Innovation 2020–Health Science and Nursing (ICoSIHSN 2020)*, Atlantis Press, 552–555.

[7] Yeni, Y., Rachmania, R., and Yanuar, M.D., 2021, *In silico* study of compounds contained in *Hemigraphis alternata* leaves against 5-LOX for anti-inflammatory, *Indones. J. Pharm. Sci. Technol.*, 8 (1), 34–41.

[8] Pires, D.E.V., Blundell, T.L., and Ascher, D.B., 2015, pkCSM: Predicting small-molecule pharmacokinetic and toxicity properties using graph-based signatures, *J. Med. Chem.*, 58 (9), 4066–4072.

[9] Boobis, A., Gundert-Remy, U., Kremers, P., Macheras, P., and Pelkonen, O., 2002, *In silico* prediction of ADME and pharmacokinetics: Report of an expert meeting organised by COST B15, *Eur. J. Pharm. Sci.*, 17 (4-5), 183–193.

[10] Brogi, S., Ramalho, T.C., Kuca, K., Medina-Franco, J.L., and Valko, M., 2020, Editorial: *In silico* methods for drug design and discovery, *Front. Chem.*, 8, 612.

[11] Chandrasekaran, B., Abed, S.N., Al-Attraqchi, O., Kuche, K., and Tekade, R.K., 2018, "Computer-Aided Prediction of Pharmacokinetic (ADMET) Properties" in *Dosage Form Design Parameters: Advances in Pharmaceutical Product Development and Research*, vol. II, Academic Press, Cambridge, United States, 731–755.

[12] Shaker, B., Ahmad, S., Lee, J., Jung, C., and Na, D., 2021, *In silico* methods and tools for drug discovery, *Comput. Biol. Med.*, 137, 104851.

[13] de Souza Neto, L.R., Moreira-Filho, J.T., Neves, B.J., Maidana, R.L.B.R., Guimarães, A.C.R., Furnham, N., Andrade, C.H., and Silva, F.P., 2020, *In silico* strategies to support fragment-to-lead optimization in drug discovery, *Front. Chem.*, 8, 93.

[14] Mvondo, J.G.M., Matondo, A., Mawete, D.T., Bambi, S.M.N., Mbala, B.M., and Lohohola, P.O., 2021, *In silico* ADME/T properties of quinine derivatives using SwissADME and pkCSM Webservers, *Int. J. Trop. Dis. Health*, 42 (11), 1–12.

[15] Pires, D.E., Kaminskas, L.M., and Ascher, D.B., 2018, "Prediction and Optimization of Pharmacokinetic and Toxicity Properties of the Ligand" in *Computational Drug Discovery and Design*, Eds. Gore, M., and Jagtap, U., pp. 271–284, Humana Press, New York, United States.

[16] Udrea, A.M., Gradisteanu Pircalabioru, G., Boboc, A.A., Mares, C., Dinache, A., Mernea, M., and Avram, S., 2021, Advanced bioinformatics tools in the pharmacokinetic profiles of natural and synthetic compounds with anti-diabetic activity, *Biomolecules*, 11 (11), 1692.

[17] Udrea, A.M., Puia, A., Shaposhnikov, S., and Avram, S.P., 2018, Computational approaches of new perspectives in the treatment of depression during pregnancy, *Farmacia*, 66 (4), 680–687.

[18] Domínguez-Villa, F.X., Durán-Iturbide, N.A., and Ávila-Zárraga, J.G., 2021, Synthesis, molecular docking, and *in silico* ADME/Tox profiling studies of new 1-aryl-5-(3-azidopropyl) indol-4-ones: Potential inhibitors of SARS CoV-2 main protease, *Bioorg. Chem.*, 106, 104497.

[19] Mansour, M.A., AboulMagd, A.M., and Abdel-Rahman, H.M., 2020, Quinazoline-Schiff base conjugates: *In silico* study and ADMET predictions as multi-target inhibitors of coronavirus (SARS-CoV-2) proteins, *RSC Adv.*, 10 (56), 34033–34045.

[20] Tripathy, D., Nayak, B.S., Mohanty, B., and Mishra, B., 2019, Solid dispersion: A technology for improving aqueous solubility of drug, *J. Pharm. Adv. Res.*, 2 (7), 577–586.

[21] Henriques, J., Falé, P.L., Pacheco, R., Florêncio, M.H., and Serralheiro, M.L., 2018, Phenolic compounds from *Actinidia deliciosa* leaves: Caco-2 permeability, enzyme inhibitory activity and cell protein profile studies, *J. King Saud Univ., Sci.*, 30 (4), 513–518.

[22] Awortwe, C., Fasinu, P.S., and Rosenkranz, B., 2014, Application of Caco-2 cell line in herb-drug interaction studies: Current approaches and challenges, *J. Pharm. Pharm. Sci.*, 17 (1), 1–19.

[23] Pecoraro, B., Tutone, M., Hoffman, E., Hutter, V., Almerico, A.M., and Traynor, M., 2019, Predicting skin permeability by means of computational approaches: Reliability and caveats in pharmaceutical studies, *J. Chem. Inf. Model.*, 59 (5), 1759–1771.

[24] Berezhkovskiy, L.M., 2007, The connection between the steady state (V_{ss}) and terminal (V_{β}) volumes of distribution in linear pharmacokinetics and the general proof that $V_{\beta} \geq V_{ss}$, *J. Pharm. Sci.*, 96 (6), 1638–1652.

[25] Guo, T., Wang, Y., Guo, Y., Wu, S., Chen, W., Liu, N., Wang, Y., and Geng, D., 2018, 1, 25-D$_3$ protects from cerebral ischemia by maintaining BBB permeability via PPAR-γ activation, *Front. Cell. Neurosci.*, 12, 480.

[26] Ju, F., Ran, Y., Zhu, L., Cheng, X., Gao, H., Xi, X., Yang, Z., and Zhang, S., 2018, Increased BBB permeability enhances activation of microglia and exacerbates loss of dendritic spines after transient global cerebral ischemia, *Front. Cell. Neurosci.*, 12, 236.

[27] Bhosle, V.K., Altit, G., Autmizguine, J., and Chemtob, S., 2017, "Basic Pharmacologic Principles" in *Fetal and Neonatal Physiology*, 5th Ed., Eds. Polin, R.A., Abman, S.H., Rowitch, D.H., Benitz, W.E., and Fox, W.W., Elsevier, Philadelphia, United States, 187–201.